**Glycobiology** vol. 19 no. 9 pp. 1034–1045, 2009
doi:10.1093/glycob/cwp084
Advance Access publication on June 18, 2009

# The α-galactomannan Davanat binds galectin-1 at a site different from the conventional galectin carbohydrate binding domain

**Michelle C Miller[2], Anatole Klyosov[3], and Kevin H Mayo[1,2]**

[2]Department of Biochemistry, Molecular Biology & Biophysics, University of Minnesota Health Sciences Center, 6-155 Jackson Hall, 321 Church Street, Minneapolis, MN 55455; and [3]Pro-Pharmaceuticals, Inc, 7 Wells Ave., Newton, MA 02459, USA

*Received on May 15, 2009; revised on June 8, 2009; accepted on June 8, 2009*

**Galectins are a sub-family of lectins, defined by their highly conserved β-sandwich structures and ability to bind to β-galactosides, like Gal β1-4 Glc (lactose). Here, we used $^{15}$N-$^{1}$H HSQC and pulse field gradient (PFG) NMR spectroscopy to demonstrate that galectin-1 (gal-1) binds to the relatively large galactomannan Davanat, whose backbone is composed of β1-4-linked D-mannopyranosyl units to which single D-galactopyranosyl residues are periodically attached via α1-6 linkage (weight-average MW of 59 kDa). The Davanat binding domain covers a relatively large area on the surface of gal-1 that runs across the dimer interface primarily on that side of the protein opposite to the lactose binding site. Our data show that gal-1 binds Davanat with an apparent equilibrium dissociation constant ($K_d$) of 10 × $10^{-6}$ M, compared to 260 × $10^{-6}$ M for lactose, and a stiochiometry of about 3 to 6 gal-1 molecules per Davanat molecule. Mannan also interacts at the same galactomannan binding domain on gal-1, but with at least 10-fold lower avidity, supporting the role of galactose units in Davanat for relatively strong binding to gal-1. We also found that the β-galactoside binding domain remains accessible in the gal-1/Davanat complex, as lactose can still bind with no apparent loss in affinity. In addition, gal-1 binding to Davanat also modifies the supermolecular structure of the galactomannan and appears to reduce its hydrodynamic radius and disrupt inter-glycan interactions thereby reducing glycan-mediated solution viscosity. Overall, our findings contribute to understanding gal-1–carbohydrate interactions and provide insight into gal-1 function with potentially significant biological consequences.**

*Keywords:* diffusion/glycan/lectin/NMR spectroscopy/protein Q

## Introduction

Galectins belong to a sub-family of lectins that bind β-galactosides, and as a group, share significant amino acid sequence conservation in their carbohydrate recognition domain (CRD) (Barondes et al. 1994). Although galectins in general are associated with intracellular functions (e.g., modulating proliferation, apoptosis, pre-mRNA splicing), they are best known for their extracellular activities in mediating cell–cell and cell–matrix adhesion and migration by interacting with various glycan groups of cell surface glycoproteins and/or glycolipids (Liu and Rabinovich 2005), whose glycan composition can even change during the life cycle of a cell (Balcan et al. 2008). Galectin-1 (gal-1) interacts with various glycoconjugate ligands of the extracellular matrix (e.g., laminin, fibronectin, β1 subunit of integrins, ganglioside GM1, and lysosomal membrane-associated proteins lamps 1 and 2), as well as those on endothelial cells (Neri and Bicknell 2005) (e.g., integrins $\alpha_v\beta_3$ and $\alpha_v\beta_5$, ROBO4, CD36, and CD13) and on T lymphocytes (e.g., CD7, CD43, and CD45) where it is known to induce apoptosis (Perillo et al. 1995, 1997). Their binding to cell surface glycoproteins can also trigger intra-cellular activity. For example, gal-1 interacts with the $\alpha_5\beta_1$ fibronectin receptor to restrict carcinoma cell growth via induction of p21 and p27 (Ras-MEK-ERK pathway) (Fischer et al. 2005).

The β(1→4)-galactoside lactose (Gal-β(1→4)-Glc) is the simplest carbohydrate to which galectins bind, and one which is used most often to delineate galectin function and structure–activity relationships in vitro (Barondes et al. 1994). In general, our structural knowledge of saccharide–galectin interactions has been limited to galectin bound with lactose (Nesmelova, Dings, et al. 2008), *N*-acetyllactosamine (Walser et al. 2004; Nagae et al. 2006), trisaccharide (Nagae et al. 2006), and an *N*-acetyllactosamine octasaccharide (Bourne et al. 1994). In all these cases, a β-galactoside-containing disaccharide moiety was shown to bind a galectin in a similar fashion at its classical CRD, and even the largest one, *N*-acetyllactosamine octasaccharide, has the remaining six saccharide units jetting out from the galectin CRD into solution, with the inference that another galectin CRD could bind the free end of the octamer to induce some type of galectin-octasaccharide polymerization.

However, glycans from various cell surface glycoproteins and glycolipids are far more complicated in situ than any of these simple model polysaccharides used to date to investigate gal-1-carbohydrate binding. Natural cell surface glycans are larger, heterogeneous in size and composition, and densely packed and therefore self-associating. Because of this, it is likely that gal-1 interacts to some extent with saccharide units other than β-galactosides in natural glycans. Werz et al. (2007) reported that although β-D-galactose comprises 23% of all terminal monosaccharides in mammalian cell surface glycans, α-D-galactose and D-mannose (in various anomeric states) comprise about 2.3% and 18.9% of them, respectively.

In the present study, we used NMR spectroscopy to investigate binding of gal-1 to a relatively large galactomannan, Davanat (weight-average molecular weight of 59 kDa) (Miller, Klyosov, et al. 2009). Davanat is composed of a

[1]To whom correspondence should be addressed: Tel: +612-625-9968; Fax: +612-612-2163; e-mail: mayox001@umn.edu

 

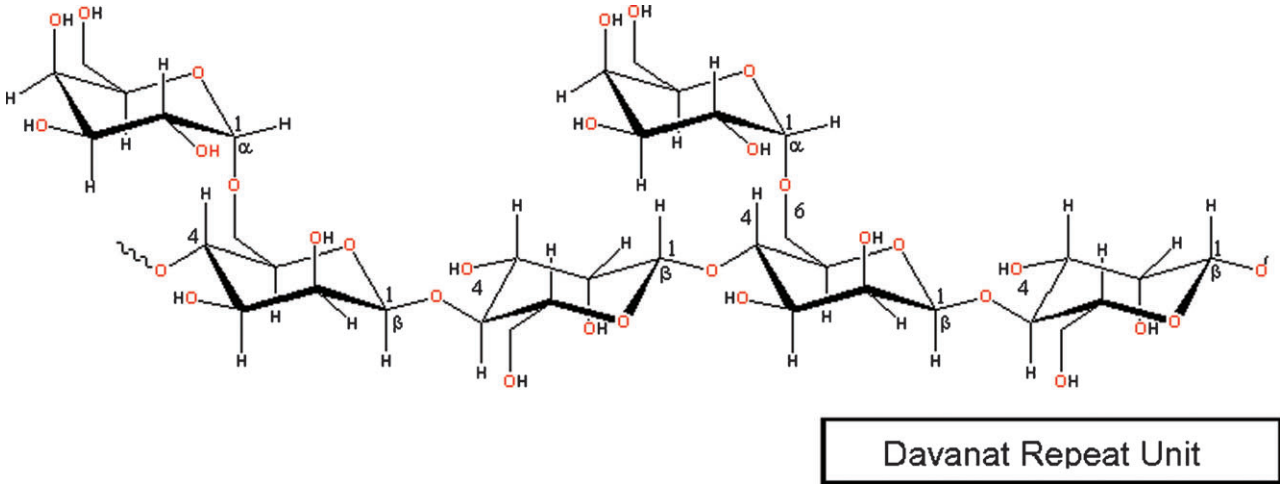


**Fig. 1.** Chemical structure of the repeat unit in Davanat. Davanat is a galactomannan, whose backbone is composed of (1→4)-linked β-D-mannopyranosyl units to which single α-D-galactopyranosyl residues are periodically attached via a (1→6)-linkage, with an average repeating unit of 17 β-D-Man residues and 10 α-D-Gal residues, and an average polymeric molecule containing approximately 12 such repeating units.

(1→4)-linked β-D-mannopyranosyl backbone to which single α-D-galactopyranosyl residues are attached via (1→6)-linkages and has a weight-average molecular weight of 59 kDa (Platt et al. 2006). A segment of a Davanat repeat unit is illustrated in Figure 1. The α-galactomannan has an average repeat unit of 17 β-D-Man residues and 10 α-D-Gal residues, with an average polymeric molecule containing approximately 12 such repeating units (Platt et al. 2006). Davanat is presently being used against metastatic colorectal cancer in Phase II clinical trials (see http://clinicaltrials.gov/ct2/show/NCT00110721).

## Results

*Gal-1 binds to Davanat*

Figure 2**A** shows a $^{1}$H-$^{15}$N HSQC spectrum of uniformly $^{15}$N-enriched gal-1 (2 mg/mL), with cross-peaks labeled as assigned previously (Nesmelova, Pang, et al. 2008). At this concentration, galectin-1 is a dimer (Barondes et al. 1994). As Davanat is added to solution, gal-1 resonances are differentially decreased in intensity (broadened), as exemplified with $^{15}$N-enriched gal-1 HSQC spectra acquired at gal-1:Davanat molar ratios of 30:1 and 15:1 (Figure 2**B** and **C**, respectively). Intensity changes are better appreciated in HSQC spectral expansions shown below each of the full HSQC spectra in Figure 2. Because all three spectra were collected, processed, and plotted the same way, it is apparent that some cross-peaks have disappeared, some are greatly reduced in intensity, and others appear relatively unperturbed. The initial conclusion from these data is that gal-1 interacts with Davanat, an α-galactomannan. The observed differential intensity change or broadening of gal-1 resonances is primarily the result of exchange between/among gal-1 and binding sites on Davanat that occurs on the intermediate chemical shift time scale (Keeler 2005). These HSQC data also indicate that the overall folded structure of the gal-1 CRD is not significantly perturbed by binding to Davanat, because even though $^{1}$H-$^{15}$N resonances are differentially broadened during the titration, chemical shifts of resonances remaining during the titration are mostly unchanged. Although this same reasoning suggests that the gal-1 dimer remains intact upon binding Davanat, we cannot state this conclusively.

*Davanat binding domain on gal-1*

By using these HSQC data, we could identify those gal-1 residues most affected by binding Davanat. We do this in a way that is similar to HSQC chemical shift mapping (Rajagopal et al. 1997), which is performed when binding interactions occur in the fast or slow exchange regimes on the chemical shift time scale. In these instances, resonances are chemically shifted, and little broadened, during the titration with ligand. In our case, gal-1 resonances initially may be shifted somewhat by the interaction with Davanat, but are primarily broadened due to the exchange process which falls in the intermediate exchange regime on the NMR chemical shift time scale (Keeler 2005). There are a number of factors that can contribute to a system falling into a particular NMR exchange regime. However, in general as a system goes from fast to intermediate to slow exchange, the life time of the complex increases, i.e., binding becomes relatively stronger.

Because interactions occurring on the intermediate exchange time scale may not show discrete resonances, the way in which we present observed broadening effects is different from the way in which we would show $^{1}$H- and $^{15}$N-weighted-average chemical shift changes for a system in the fast or slow exchange regimes. In the intermediate exchange regime, we show differential broadening at a molar ratio where most resonances are still observed, but are at lower intensities due to broadening. We refer to this as HSQC resonance broadening mapping to distinguish it from HSQC chemical shift mapping. The interpretation is essentially the same as with HSQC chemical shift mapping, i.e., those resonances that are initially broadened the most are associated with that site(s) on gal-1 that interacts with Davanat. In general, fractional changes are calculated by subtracting from one the intensity of a given HSQC cross-peak divided by that in pure gal-1 at the same protein concentration. A value of 1 indicates that a resonance is no longer apparent, and a value of zero indicates no change in resonance intensity. We create the HSQC resonance broadening map by taking fractional changes in gal-1

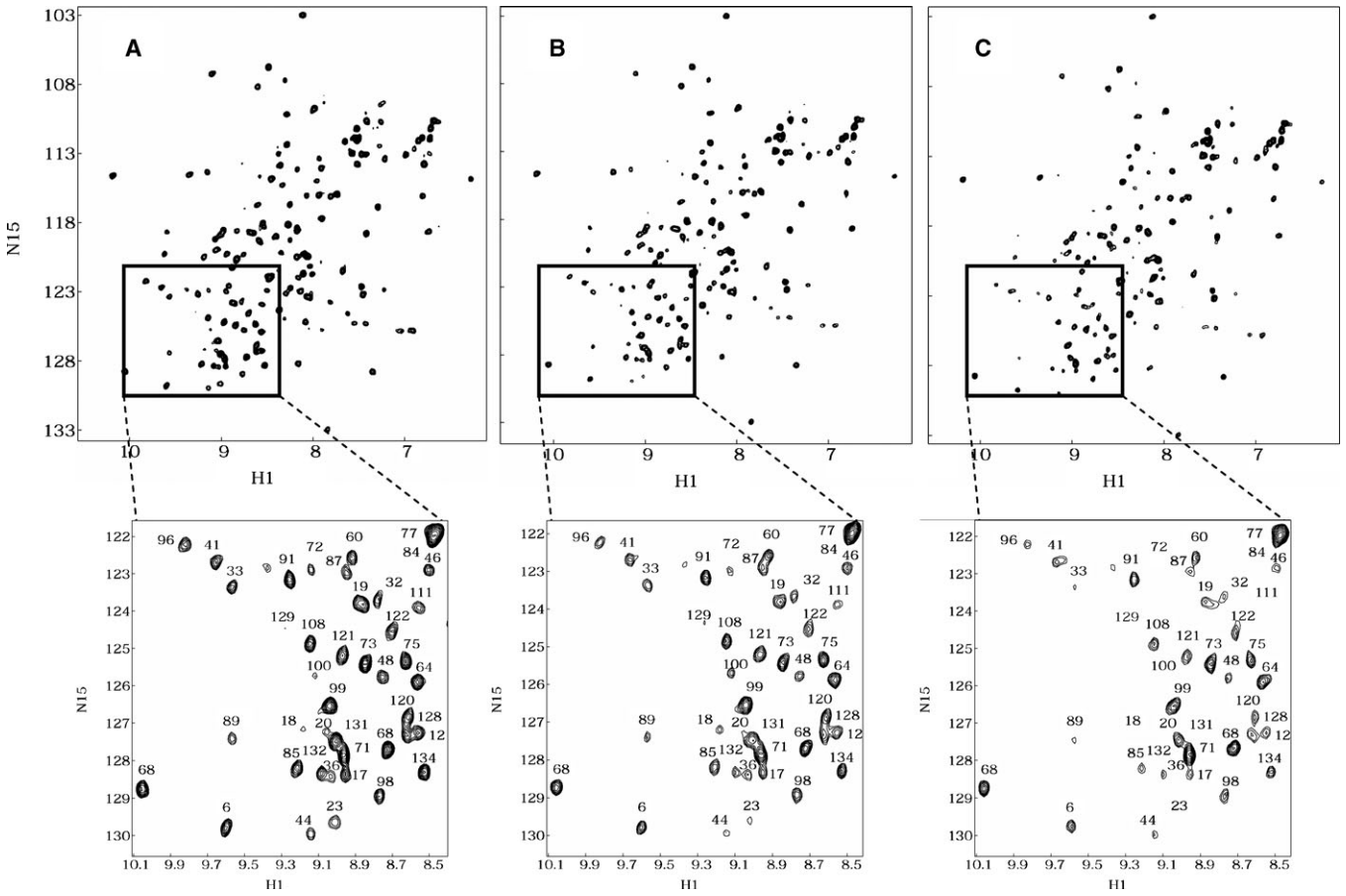


**Fig. 2.** $^{1}$H-$^{15}$N HSQC spectra for gal-1 with and without Davanat. HSQC spectra are shown for $^{15}$N-enriched gal-1 (1 mg/mL) alone (**A**) and at gal-1:Davanat molar ratios of 30:1 (**B**) and 15:1 (**C**). Spectral expansions are provided below each plot to better visualize the observed resonance broadening as Davanat is added to the gal-1 solution. Resonances in the expansion plots are labeled with assignments reported by Nesmelova, Pang, et al. (2008).

HSQC resonance intensities observed at a low Davanat:gal-1 molar ratio (where most gal-1 resonances are still apparent) and by plotting them versus the amino acid sequence of gal-1. This is illustrated in Figure 3. Clearly, some gal-1 residues are more affected than others.

Gal-1 has a β-sandwich structure that comprises 11 β-strands identified in Figure 3. The lactose binding face of gal-1 has β-strands 1, 10, 3, 4, 5, and 6, in that order with strand 1 at the dimer interface. The lactose binding domain itself primarily involves β-strands 4, 5, 6, 9, and interconnecting loops. The opposite face of gal-1 starts with β-strand 11 at the dimer interface (and across from β-strand 1 in the β-sandwich), followed by β-strands 2, 7, 8, and 9. From Figure 3, note that residues within the lactose binding domain are generally least affected by the presence of Davanat, whereas residues on the opposite face are on average most affected. This is perhaps better appreciated in Figure 4**A**, which highlights the most affected residues on the structure of the gal-1 dimer. The region with which Davanat interacts is on the face of gal-1 opposite to where lactose binds (Figure 4**A**, right) and comprises a rather broad swath that traverses the gal-1 dimer interface.

The residues most affected are L9, N10, G14, R18, R20, G21, V23, K28, N33, L34, K36, N46, I58, G69, Q80, G82, A85, C88, I89, F91, D92, L96, L100, D102, Y104, R111, N118, K129, C130, A132, and F133. The side-chains of these residues are illustrated in the gal-1 dimer in Figure 4**B**. Overall, the amino acid residue composition is quite similar to that of the lactose binding site, where key residues are primarily polar (N46, N61, H44, R48, H52, E71) or hydrophobic (W68). Because intermediary exchange broadening made it difficult to perform $^{15}$N- or $^{13}$C-edited NOESY to identify NOEs between groups on the protein and glycan, we can only suggest the potential for similar types of protein–glycan interactions, namely hydrogen bonding and hydrophobic interactions.

Our HSQC data can also be used to estimate the gal-1/Davanat apparent binding affinity by plotting the average fractional change in gal-1 HSQC resonance intensities as a function of Davanat concentration, as shown in the inset to Figure 3, with the solid line showing the fit to the data. An apparent $K_d$ value is estimated at the point on this curve where 50% of the gal-1 molecules are bound to Davanat. The average fractional intensity change of 0.5 (50% bound) occurs at a Davanat concentration of 0.5 mg/mL, which corresponds to an apparent $K_d$ value of about $10 \times 10^{-6}$ M using the 59 kDa weight-average molecular weight of Davanat (Miller, Klyosov, et al. 2009). This value represents a weighted average over all binding sites on the glycan and is consistent with observed resonance broadening that places the system in the intermediate exchange regime on the chemical shift time scale (Keeler 2005).

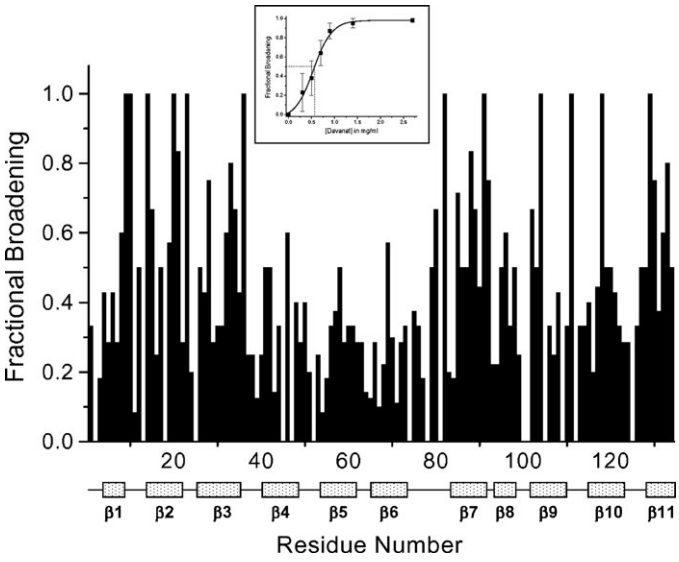


**Fig. 3.** Gal-1/Davanat binding from HSQC resonance broadening map. Fractional changes in gal-1 resonance intensities observed at a gal-1:Davanat molar ratio (20:1) where most gal-1 resonances are still apparent versus the amino acid sequence of gal-1. A value of 1 indicates that the resonance associated with that particular residue is no longer apparent, and a value of zero indicates no change in resonance intensity. The 11 β-strands in gal-1 are identified below the residue number. The inset shows the average fractional change (±SE) in gal-1 HSQC resonance intensities versus the concentration (mg/mL) of Davanat. The solid line represents a sigmoidal fit to the average of these values at each point.

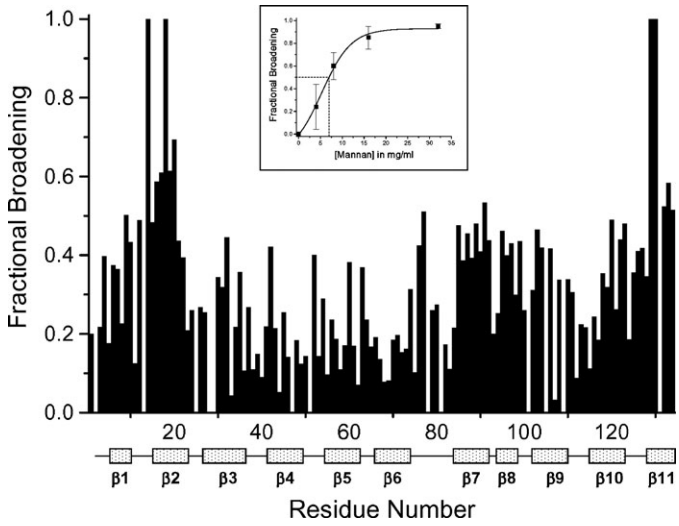


**Fig. 5.** HSQC resonance broadening map for binding of mannan to gal-1. Fractional changes in gal-1 (4 mg/mL) HSQC resonance intensities in the presence of mannan (16 mg/mL) versus the amino acid sequence of gal-1. A value of 1 indicates that the resonance associated with that particular residue is no longer apparent, and a value of zero indicates no change in resonance intensity. The 11 β-strands in gal-1 are identified below the residue number. The inset shows the average fractional intensity change (±SE) of cross-peaks versus the mannan concentration (mg/mL). The solid line represents a polynomial fit to these data.

*Gal-1 also binds to mannan*

To assess whether galactose units in Davanat were necessary to gal-1 binding, we performed $^{1}H$-$^{15}N$ HSQC experiments on $^{15}N$-enriched gal-1 in the presence of a mannan (weight-average molecular weight of 50 kDa) at concentrations of 4, 8, 16, and 32 mg/mL. We observed that mannan broadened gal-1 resonances in a similar fashion as Davanat. Figure 5 shows an HSQC resonance broadening mapping which plots gal-1 HSQC cross-peak intensities versus the amino acid sequence. As with Figure 3 for Davanat, a value of 1 indicates that the resonance associated with that particular residue is no longer apparent, and a value of zero indicates no change in resonance intensity. Although mannan binding mostly affects β-strands 2 and 11 on gal-1 (Figure 5), a comparison of Figures 3 and 5 shows that mannan and Davanat generally bind at the same region on gal-1.

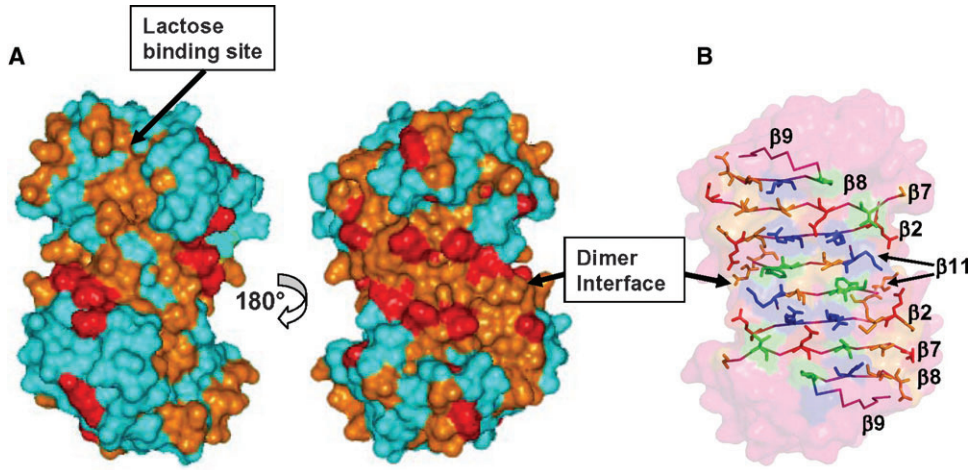


**Fig. 4.** Davanat binding domain on gal-1. (**A**) Residues on the folded structure of gal-1 that have been most affected by binding to Davanat are highlighted in red and orange as discussed in the text. The x-ray structure of lactose-bound human galectin-1 has been used in this figure (pdb access code: 1gzw, Lopez-Lucendo et al.) (2004). The orientation at the left shows the face of the dimer where Davanat binds. The gal-1 dimer interface is also indicated. The orientation at the right shows the opposite side of the dimer where lactose binds. (**B**) Illustration of gal-1 residues in the Davanat binding domain. Polar, positively charged, and hydrophobic residues are colored in orange, blue, and green, respectively. For reference, the lactose molecule in its binding site is shown in purple.

Nevertheless, gal-1 binds mannan considerably more weakly than it does Davanat. The inset to Figure 5 plots the average intensity change of cross-peaks from the most affected residues versus the mannan concentration. At a fractional intensity change of 0.5 (50% gal-1 bound), the mannan concentration is about 7 mg/mL, which corresponds to an apparent $K_d$ value of about $140 \times 10^{-6}$ M using a 50 kDa weight-average molecular weight for this mannan preparation. This value is 14-fold larger than that found for Davanat ($10 \times 10^{-6}$ M), indicating that mannan binding to gal-1 is about 14-fold weaker than Davanat.

*Lactose can bind the gal-1/Davanat complex*

We confirmed that Davanat does not interact directly with the β-galactoside binding site on gal-1 by demonstrating that lactose can still bind at this site in the gal-1/Davanat complex. For this experiment, we started with a solution of $^{15}$N-gal-1:Davanat (molar ratio of 10:1), added lactose at concentrations of 1, 3, and 10 mM, and acquired $^{1}$H-$^{15}$N HSQC spectra at each point in the titration. We used a gal-1:Davanat molar ratio of 10:1 where much of the gal-1 is unbound because otherwise there would be little or no NMR signal to observe due to broadening from chemical exchange on the intermediate chemical shift time scale. We did perform the experiment at a 5:1 gal-1:Davanat molar ratio, and lactose still bound, although we could not follow chemical shifts of many of the gal-1 cross-peaks due to their absence from the spectrum (data not shown).

Figure 6**A** overlays HSQC spectral expansions for $^{15}$N-gal-1:Davanat (10:1) and the three lactose additions. The HSQC spectrum for $^{15}$N-gal-1:Davanat without lactose (black cross-peaks) is essentially the same as that shown in Figure 2**C**, where resonances are differentially broadened (reduced in intensity or not observed, e.g., N46, E74, D92 in Figure 6**A**), as described above. Although cross-peak intensities, e.g., for N46 and D92 are highly attenuated, they are evident at lower levels in the spectrum (not shown). As lactose is added (magenta for 1 mM, red for 3 mM, and blue for 10 mM), these resonances generally tend to increase in intensity and are the most highly shifted in this expansion region, as highlighted with the dashed boxes.

Lactose-induced chemical shift changes for N46, E74, and D92 in the gal-1/Davanat complex are essentially the same as those observed with gal-1 alone at the same lactose concentrations (Figure 6**B**). In fact, the same can be said for all gal-1 cross-peaks, as illustrated by HSQC chemical shift maps shown in Figure 6**C** and **D**. A linear fit of shift changes in one case plotted versus the other yields a regression coefficient of 0.94, indicating that lactose binds essentially the same way to its quintessential binding site in the gal-1/Davanat complex, as it does to that site in gal-1 alone.

We also found that lactose binding affinities are essentially the same for free gal-1 and for the gal-1/Davanat complex, as illustrated in Figure 6**E** and **F** where we plot fractional changes in gal-1 $^{1}$H-$^{15}$N-weighted HSQC resonance chemical shifts as a function of the lactose concentration in the presence and absence of Davanat, respectively. The solid line represents a sigmoidal fit through average values at each lactose concentration point. $K_d$ values were estimated at that point on either curve where 50% of the gal-1 binding sites are occupied with lactose (0.5 fraction bound). $K_d$ values are essentially the same, namely $250 \times 10^{-6}$ M.

In either case because gal-1 resonances are simply shifted by the addition of lactose, ligand exchange at the β-galactoside binding site is relatively fast on the chemical shift time scale. With Davanat, however, ligand exchange occurs on a relatively slower time scale (intermediate chemical exchange), as evidenced by the presence of gal-1 resonance broadening discussed in the previous section. Now, when lactose binds the gal-1/Davanat complex, the Davanat-induced broadening is initially somewhat reduced, i.e., resonance intensity increases, suggesting that lactose binding induces somewhat lower affinity or avidity of gal-1 for Davanat. This is exemplified in Figure 6**A**, in particular with the behavior of resonances for N46 and D92 and to a lesser extent with E74. The cross-peak for N46 is not even apparent prior to the addition of 1 mM lactose, after which it is increased in intensity (compare with N46 intensity in Figure 6**B**). The D92 resonance is increased in intensity only at 1 mM lactose.

Similar trends are noted for other gal-1 resonances, as illustrated in Figure 7**A** which shows HSQC resonance broadening maps for gal-1:Davanat (10:1) in the absence (top) and presence (bottom) of 1 mM lactose. As with Figure 3**B**, a value of 1 indicates that the resonance associated with that particular residue is no longer apparent, and a value of zero indicates no change in resonance intensity. A simple average in fractional broadening over all residues in the gal-1:Davanat complex (Figure 7**A**) goes from 0.72 in the absence of lactose to 0.51 in the presence of 1 mM lactose. Most gal-1 resonances behave like D92 (Figure 6**A**), as illustrated in Figure 7**B** which plots trends for 28 other residues. In this regard, resonance broadening is diminished upon the addition of 1 mM lactose, and then is increased again as more lactose is added to the solution. In either instance, gal-1 remains bound to Davanat, as indicated by sustained gal-1 resonance broadening. To some extent, lactose binding to the gal-1/Davanat complex apparently modulates affinity of gal-1 for Davanat, which suggests that when lactose binds the complex, gal-1 undergoes a conformational transition, however minor.

One concern we had with the interpretation of simultaneous binding was that for technical reasons we had to use a gal-1:Davanat molar ratio of 10:1, such that much of the gal-1 was unbound. Therefore, we could be observing lactose binding to free gal-1. However, the Davanat/gal-1/lactose system is continually exchanging, and the effect we observe should be the result of some weighted averaging. Moreover, the lactose concentration was taken up to greater than saturating levels, and Davanat remained bound to gal-1, as evidenced by sustained gal-1 resonance broadening in the presence of Davanat and lactose. In this regard, it does appear that lactose and Davanat can bind gal-1 simultaneously.

*From the glycan side*

In our NMR experiments, we actually observe an average effect from gal-1 binding to glycans in the Davanat preparation that vary somewhat in size (Miller, Klyosov, et al. 2009). Therefore, we performed pulse field gradient (PFG) NMR diffusion experiments to derive diffusion coefficients, $D$, for insight into what occurs from the perspective of glycan molecules when they bind gal-1. For the most part, changes in $D$-values reflect changes in molecular size (apparent molecular weight and hydrodynamic radius) and/or solution viscosity due to intermolecular

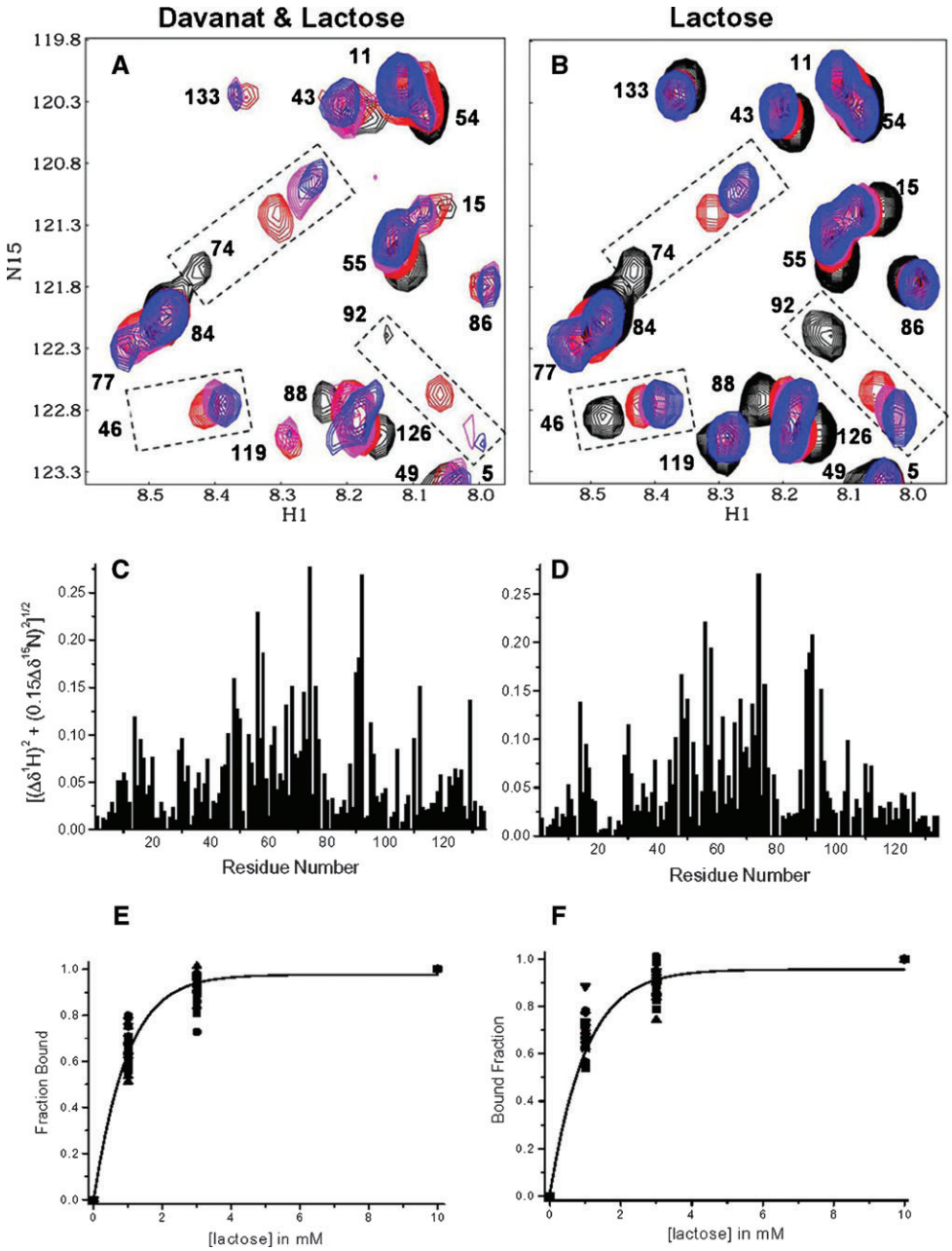


**Fig. 6.** Lactose binds gal-1 in presence of Davanat. (**A**) Overlay of expansions from two HSQC spectra of $^{15}$N-enriched gal-1 (1 mg/mL) in the presence of Davanat (molar ratio of 10:1, gal-1:Davanat) (black cross-peaks) and with the addition of lactose at 1 mM (magenta), 3 mM (red), and 10 mM (blue). (**B**) Overlay of expansions from two HSQC spectra of $^{15}$N-enriched gal-1 (1 mg/mL) alone (black cross-peaks) and with the addition of lactose at 1 mM (magenta), 3 mM (red), and 10 mM (blue). Resonances in expansion plots in **A** and **B** are labeled as assigned previously by Nesmelova, Pang, et al. (2008). (**C**) $^{15}$N-$^{1}$H-weighted chemical shift differences ($\Delta\delta$) of gal-1 resonances observed upon the addition of lactose to a solution of gal-1 containing Davanat as in **A** versus the amino acid sequence of gal-1. (**D**) $^{15}$N-$^{1}$H-weighted chemical shift differences ($\Delta\delta$) of gal-1 resonances observed upon the addition of lactose to a solution of gal-1 alone as in **B** versus the amino acid sequence of gal-1. (**E**) The fractional chemical shift changes of the 20 most shifted resonances of gal-1 in the presence of Davanat (from data as exemplified in **A**) as a function of lactose concentration. (**F**) The fractional chemical shift changes of the 20 most shifted resonances of gal-1 alone (from data as exemplified in **B**) as a function of lactose concentration. The solid lines in both **E** and **F** represent sigmoidal fits to the averages of these values at each point, as discussed in the text.

interactions among these "sticky" glycans (Daas et al. 2000). A smaller *D*-value generally indicates an increase in molecular size and/or viscosity, and *vice versa*. In addition, because polysaccharides generally have no stable globular core, *D*-values for Davanat may also depend on internal motion to a greater degree than for a protein, whereby greater internal flexibility is reflected in a larger *D*-value.

For these NMR diffusion experiments, we maintained the concentration of Davanat at 4.6 mg/mL, titrated gal-1 into the glycan solution, and observed effects on *D* derived from gradient-induced decay or dephasing of $^{1}$H resonances from Davanat. A $^{1}$H NMR spectrum of Davanat is shown in Figure 8**A**. Although knowledge of specific resonance assignments is not necessary to our analysis, the range of $^{1}$H chemical

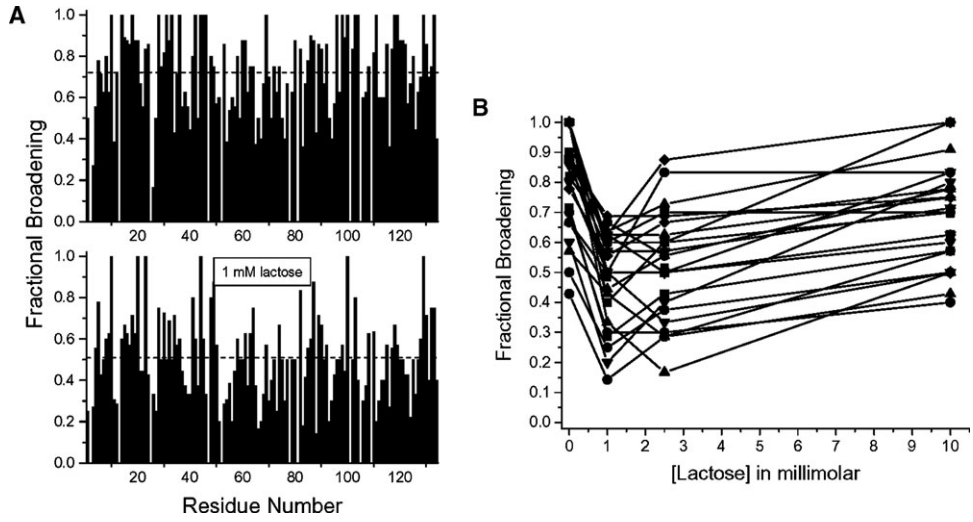


**Fig. 7.** Lactose reduces Davanat-induced broadening. (**A**) The top plot shows fractional changes in resonance intensities of gal-1 in the presence of Davanat (molar ratio of 10:1 gal-1:Davanat) versus the amino acid sequence of gal-1. A value of 1 indicates that the resonance associated with that particular residue is no longer apparent, and a value of zero indicates no change in resonance intensity. The bottom plot shows fractional changes in resonance intensities of gal-1 in the presence of Davanat (molar ratio of 10:1 gal-1:Davanat) and 1 mM lactose versus the amino acid sequence of gal-1. (**B**) Fractional broadening for 28 resonances of gal-1 in the presence of Davanat is plotted versus the lactose concentration. Lines shown simply connect data points as visual aids.

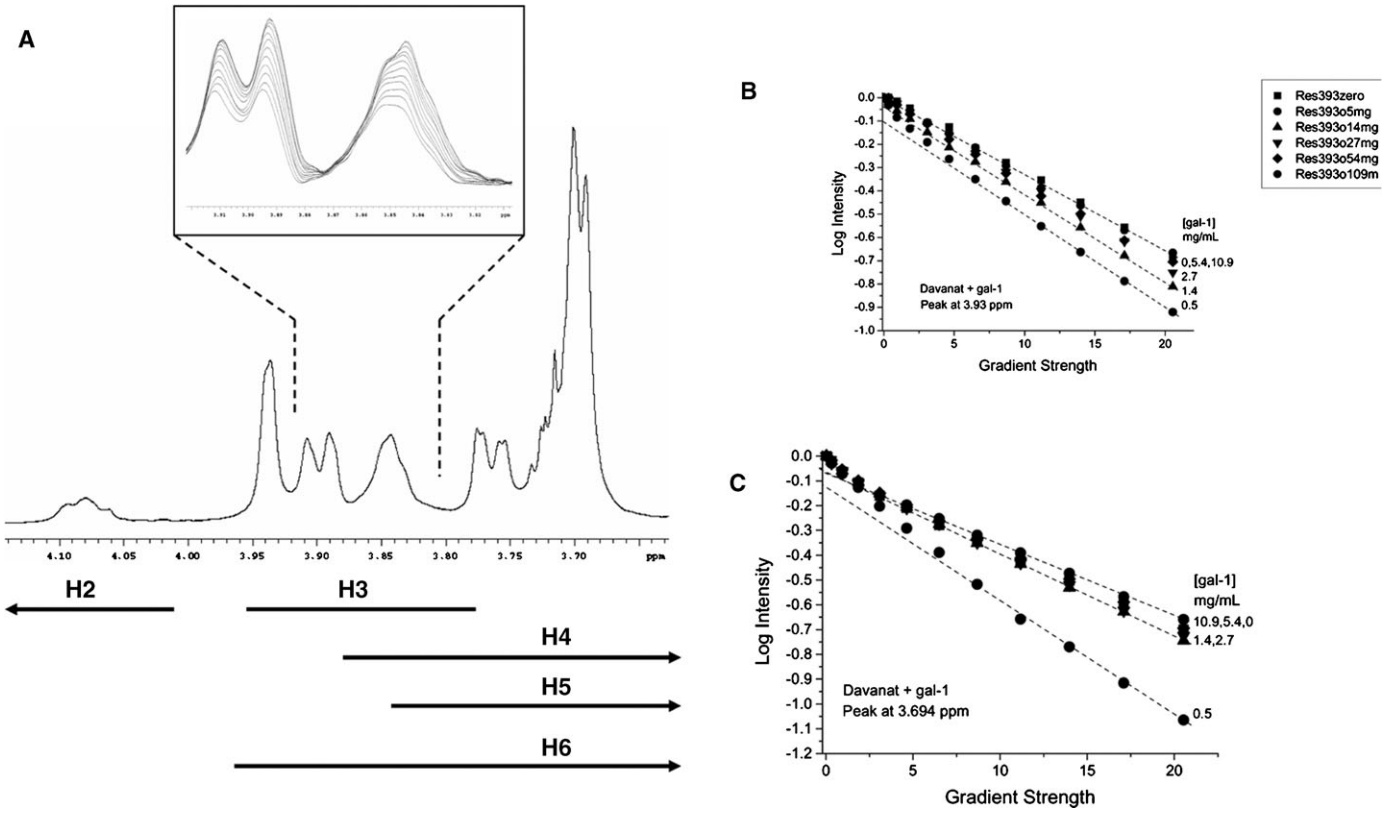


**Fig. 8.** $^{1}$H NMR of Davanat, along with diffusion decay curves for titration with gal-1. (**A**) A $^{1}$H NMR spectral trace for Davanat is shown. The inset illustrates the diffusion-mediated gradient-induced decay of a few resonance envelopes as discussed in the text. Lines below the spectrum provide ranges for chemical shifts of protein resonances for Gal and Man rings, as discussed in the text. Diffusion decay curves for Davanat resonances at 3.93 ppm (**B**) and 3.694 ppm (**C**) are shown as a function of the gal-1 concentration in mg/mL. The glycan concentration was held constant at 4.6 mg/mL, and gal-1 was titrated into solution. Dashed lines show extrapolation to the Y-intercept of the slow component of the decay curve, as discussed in the text.

shifts expected for the various chemical groups in this galactomannan is indicated below the spectrum, as complied from a number of studies (Ikuta et al. 1997; Taguchi et al. 1997; Ishrud et al. 2001; Takita et al. 2001; Rakhmanberdyeva and Shashkov 2005). Anomeric $^1$H resonances (not shown) are found at 4.69–4.78 ppm for mannose and 4.98–5.06 ppm for galactose.

The inset to Figure 8**A** exemplifies how resonances decay as a function of increasing gradient strength according to Eq. (1) (see *Material and methods*), with the most intense resonance at the start of the measurement when the gradient strength is zero. As the gradient strength is increased, resonances become more dephased and therefore decrease in intensity. If Davanat were composed of single-sized glycan molecules and internal motional differences were absent, *D*-values derived from individual resonances that represent different chemical groups within the glycan molecule would be the same or very nearly the same. However, Davanat is a polydispersed polysaccharide (Miller, Klyosov, et al. 2009), and for reasons mentioned above, *D*-values do vary depending upon which Davanat resonance was used to derive a given *D*-value. This is evident in the inset to Figure 8**A** where gradient-induced dephasing within the resonance envelope around 3.83–3.86 ppm is not uniform. It is for this reason that we measured diffusion-mediated decay curves for several of the Davanat resonances.

By plotting the logarithm of the fractional change in $^1$H resonance intensity (resonance intensity divided by the initial intensity at zero gradient) versus gradient strength, one obtains decay curves whose slopes yield diffusion coefficients, *D* (see *Material and methods*, Eq. 1). Figure 8**B** and **C** show decay curves for two resonances of Davanat (3.7 ppm and 3.94 ppm) as a function of increasing gal-1 concentration (indicated at the right of each curve). For pure Davanat, the decay curve for the resonance at 3.94 ppm (Figure 8**B**) appears linear, whereas that for the resonance at 3.7 ppm (Figure 8**C**) is slightly curvilinear. Decay curves appear linear when *D*-values vary only by about 5–10%. Similar variations are observed for decay curves from other Davanat resonances. For curvilinear decay curves, we can estimate the fraction of the slow decay component from the Y-intercept, if we assume the presence of only two species. Dashed lines in Figure 8**A** and **B** are shown through the final 6–8 points of the curves to indicate the slow decay components. Linear fits to these points are very good, with regression coefficients greater than 0.9. The fractional contribution of these slow components to the full decay curves can be estimated from the Y-intercept of the linearly extrapolated curves (dashed lines). In general, we find that the fast and slow decay components account for about 10 and 90%, respectively, of individual curvilinear decay curves. Because the fraction of the "fast component" is minimal, we focused our analysis on the slower component. The presence of the "fast component" could result from increased internal motions of various carbohydrate units within Davanat.

When the initial aliquot of gal-1 (0.5 mg/mL) is added to the Davanat solution, the slope of a slow decay component increases greatly (Figure 8**B** and **C**), corresponding to a dramatic increase in *D*. This trend is reversed by subsequent additions of gal-1 that lead to less steep decay curves and therefore decreases in *D*. In Figure 9, we plot *D*-values for the major resonances of Davanat as a function of the concentration of gal-1. Regardless of the resonance, we observe that *D*-values usually increase initially upon the addition of gal-1, and then decrease at higher gal-1:Davanat molar ratios, before tending to level off. At that point

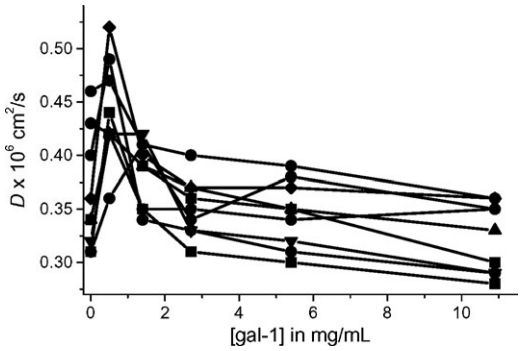


**Fig. 9.** Diffusion coefficients for Davanat. (**A**) *D*-values for the slow component of the deconvoluted diffusion decay curves are plotted versus gal-1 concentration. (**B**) Lines indicating diffusion coefficients for standard glycans and proteins versus their molecular weights are shown as discussed in the text. The dashed line indicates a hypothetical situation for protein bound to glycan, where the complex is neither protein nor glycan, but some combination of both.

where these curves tend to level off (gal-1 concentration of 3 to 6 mg/mL or $207 \times 10^{-6}$ M to $414 \times 10^{-6}$ M, respectively), we can estimate binding stoichiometry. With the Davanat concentration at 4.6 mg/mL ($78 \times 10^{-6}$ M), an average molecule of Davanat would be able to bind about 3 to 6 gal-1 monomer equivalents.

The initial sharp increase in *D* occurs at about a gal-1:Davanat molar ratio of 1:2, and then falls prior to reaching a molar ratio of 1:1. At these initial gal-1 concentrations, most of the gal-1 should be bound to the glycan (vis-a-vis our NMR HSQC data presented above), yet *D*-values increase, suggesting the opposite. Some likely explanations for this apparent conundrum are that (1) gal-1 binding disrupts the extensive inter-glycan network that contributes to the normally high solution viscosity of the Davanat solution, (2) the hydrodynamic radius of the glycan is decreased by gal-1 binding, and/or (3) gal-1 binding increases internal flexibility of the glycan molecules. In any event, gal-1 binding alters Davanat conformation and likely perturbs inter-glycan interactions.

## Discussion

Here, we report that gal-1 binds an α-galactomannan (Davanat) and an oligomannan at a site that is distinct from the galectin β-galactoside binding domain. Davanat, which is composed of (1→4)-linked β-D-mannopyranosyl units to which single α-D-galactopyranosyl residues are attached via (1→6)-linkages (Platt et al. 2006), binds gal-1 over a broad swath that traverses the dimer interface on that side of the protein opposite the β-galactoside binding domain. The presence of numerous polar residues within this carbohydrate binding domain is consistent with it being able to promote protein–glycan interactions. Moreover, it appears that this binding domain could accommodate a mannan backbone chain length of about 10 saccharide units that wrap around the surface of gal-1, much as was found for heparin binding to platelet factor-4 (Mikhailov et al. 1999). The binding of gal-1 to this α-galactomannan (Davanat) and oligomannan in this fashion is surprising given results from other studies using mannose or oligomannans. In the x-ray crystal structure of mannose-bound gal-10, the monosaccharide clearly interacts at the normal β-galactoside binding domain, albeit somewhat differently from, e.g., lactose (Swaminathan et al. 1999). In two

other studies, gal-3 was shown to bind β-1,2-linked oligomannans, either on the surface of *Candida albicans* or conjugated to bovine serum albumin (Fradin et al. 2000; Kohatsu et al. 2006). However, in one of those studies (Fradin et al. 2000), β-1,2-linked oligomannan could not be competed off by lactose, suggesting that the oligomannan bound to gal-3 at a site other than the β-galactoside binding domain. Moreover, in the other study (Kohatsu et al. 2006), even 100 mM lactose did not completely eliminate binding of gal-3 to β-1,2-linked oligomannans on the surface of *C. albicans*. Here, we observed that lactose and an α-galactomannan can bind simultaneously to gal-1, indicating the presence of two carbohydrate binding domains on gal-1. In this regard, it may be that β-1,2-linked oligomannans also bind to an analogous secondary binding site on gal-3. Many of the amino acid residues within the α-galactomannan (Davanat) binding domain on human gal-1 are conserved in sequences of other galectins (Nesmelova, Dings, et al. 2008).

We also found that mannan devoid of galactose bound gal-1 with significantly reduced affinity compared with the α-galactomannan Davanat ($K_a = 1 \times 10^5$ $M^{-1}$ for Davanat, compared to $0.7 \times 10^4$ $M^{-1}$ for mannan). This suggests that galactose units in the context of this mannan backbone promote greater binding affinity to gal-1. However, it remains unknown whether galactose must be attached to the mannan via an α(1→6)-linkage, as in Davanat. It has been reported that gal-1 binds better to some α-galactosides than to their β-anomers (Appukuttan et al. 1995). Appukuttan (2002) found that gal-1 bound to natural glycoproteins, artificially glycosylated proteins, and oligosaccharides containing terminal α-linked galactose (normally α(1→3) in these oligos) more strongly than to oligos with terminal β-linked galactose. In addition, Wu et al. (2006) reported that gal-5 bound more strongly to some blood group oligosaccharides when an α(1→x)-galactose was added to the terminal Galβ1-4GlcNAc or Galβ1-3GlcNAc core oligosaccharides and that the carbohydrate binding domain was composed of a shallow groove large enough to accommodate a pentasaccharide with an α-anomeric galactose.

The binding of gal-1 to Davanat and mannan at this nontraditional carbohydrate binding domain prompts the question of biological relevance. While we have no direct answer, we do know that gal-1 function is related to its ability to bind to glycans on the extracellular matrix and cell surface (Perillo et al. 1995, 1997; Fischer et al. 2005; Neri and Bicknell 2005), and our study does expand the view of how gal-1 may interact with cell surface glycans. Our results also demonstrate that lactose can still bind to the gal-1/Davanat complex at its quintessential β-galactoside binding site, with no apparent change in its affinity for the CRD. Nevertheless, lactose is not the in vivo ligand for gal-1, and binding to biologically more relevant oligosaccharide structures/ligands could very well be influenced by Davanat. In any event, it is interesting to propose that this dual mode of the gal-1/glycan interaction may facilitate glycan cross-linking in situ, as many different saccharides comprise mammalian cell surface glycans (Werz et al. 2007). For example, while β-D-galactose comprises 23% of all terminal monosaccharides, α-D-galactose comprises 2.3% of them, and D-mannose, in one anomeric state or another, comprises 18.9%, with terminal α-D-mannose residues coming in at 8.2%. Moreover, the composition of cell surface glycans continually changes during the life of a cell (Balcan et al. 2008; Laughlin et al. 2008; Rodgers et al. 2008), as well as being dependent upon its pathological state (Fukuda 1996; Daniels et al. 2002; Kannagi et al. 2004) and temporal/spatial dynamics (Rabinovich et al. 2007).

Davanat has been developed as a therapeutic intervention against cancer (see http://clinicaltrials.gov/ct2/show/NCT00110721), and we demonstrated here that Davanat interacts with gal-1 which is known to be crucial to tumor growth via promotion of tumor endothelial cell adhesion and migration (Thijssen et al. 2006). Even though Davanat does not greatly influence carbohydrate binding at the quintessential β-galactoside binding site on gal-1 nor does it significantly perturb the gal-1 monomer structure or apparently dimer stability, its mechanism of action could be explained by simply sequestering gal-1 to perturb normal gal-1 mass action, or by inducing changes in the microenvironment around gal-1 and cell surface glycans, or by affecting the gal-1-glycoconjugate supramolecular structure. Any of these could influence gal-1 function in terms of cell adhesion/migration, glycan cross-linking, and/or glycoconjugate receptor signaling.

Gal-1 binding to Davanat clearly affects physicochemical properties of the glycan in solution. As with all oligosaccharides in aqueous solution, galactomannans like Davanat are viscose, even at low concentration due to their high hydrodynamic volume (Daas et al. 2000). The relatively high viscosity results from the mannan backbone concentration and is independent of the galactose content which apparently determines overall solubility. *D* is related to the molecular size (apparent weight-average molecular weight and hydrodynamic radius). At infinite dilution, Davanat exhibits an average *D*-value that reflects an apparent weight-average molecular weight of 59 kDa (Miller, Klyosov, et al. 2009). At the start of the titration with gal-1, Davanat at 4.6 mg/mL (Figure 8) has a *D*-value that reflects an apparent molecular weight of 110 kDa due to intermolecular interactions among glycan molecules. The addition of small amounts of gal-1 causes *D* for Davanat to increase. This observation seems to contradict the fact that gal-1 binds the glycan, which should have resulted in a decrease in *D*. The onset of this effect occurs when only one or a few gal-1 binding sites on an average molecule of Davanat become occupied. Although it is unclear how this occurs on the molecular level, it is likely that gal-1 binding reduces intermolecular interactions among glycan molecules, which is fundamental to glycan-induced viscosity. The initial increase in *D* could also result from a drop in the hydrodynamic radius (and to some extent an increase in internal flexibility) of the glycan when it becomes complexed with small amounts of gal-1. Using the Stokes–Einstein relationship (Cantor and Schimmel 1980), the change in $R_H$ would be about 78–51 Å, which would be an appreciable change in molecular volume. In this respect, it is most likely that some combination of a change in $R_H$ and decrease in inter-glycan interactions (i.e., reduced solution viscosity) is occurring. As the titration continues, *D*-values then decrease as more and more gal-1 is bound to the glycan and levels off as binding saturation occurs. Nevertheless, gal-1 binding to Davanat causes the supermolecular structure of the glycan to be changed, attenuates inter-glycan interactions, and results ultimately in glycan decongestion. We have observed this phenomenon previously in gal-1 binding studies with a large heterogeneous galactorhamnogalacturonate glycan (Miller, Nesmelova, et al. 2009).

Galectin-mediated glycan decongestion may be biologically relevant. For example, the cell surface packing density for glycan-containing mucins in a plasma membrane is about

50 molecules/$\mu m^2$, which (assuming a cube of about $10^{-6}$ m on each side) corresponds to a peptidoglycan concentration of about $10^{-5}$ M on the cell surface (Rabuka et al. 2007, 2008). Considering that glycoproteins are not generally homogeneously dispersed on the cell surface and are often found in microdomains, the concentration for some glycoproteins (and their associated glycans) can be quite high, and therefore glycan microviscosity at the cell surface can be at or approaching what we are investigating here with these galactomannans. In terms of biological function, gal-1 is integrally involved in cell adhesion and migration, and cell adhesion generally occurs by changing the organization of cell surface glycoproteins and by antagonizing the effect of protein adhesion systems (Brewer et al. 2002; Taylor and Drickamer 2007). Gal-1 interactions with cell surface glycans are certainly known to alter membrane properties, as it does here with Davanat. Gupta et al. (2006) demonstrated using erythrocytes and EPR spectroscopy that gal-1 significantly increases membrane fluidity, which is inversely correlated with viscosity. In addition, confocal microscopy has demonstrated that upon exposure to gal-1, CD45 and CD43 are observed to cluster on the cell surface of MOLT-4 cells (leukocytes) within 20 min upon exposure to gal-1 (Pace et al. 1999). A similar observation has been made with gal-3, which has been shown to associate and form clusters when it interacts with cell surface glycans, thereby explaining its ability to mediate reorganization of cell surface glycoproteins (Nieminen et al. 2007). Taken together, these data suggest that gal-1 interacts with cell surface glycans and allows reorganization to occur, perhaps by promoting dissociation of glycoproteins via binding of gal-1 to their glycans and promoting greater membrane fluidity by decreasing glycan-mediated microviscosity. This would be analogous to decongesting a traffic jam and allowing more free diffusion within the plane of the cell membrane to occur.

## Conclusions

Here, we contradict galectin dogma by demonstrating that gal-1 binds to the α-galactomannan Davanat at a novel carbohydrate binding domain on the side of gal-1 opposite to where β-galactosides bind. Our observation that the β-galactoside lactose can still bind to the gal-1/Davanat complex suggests that gal-1-mediated glycan cross-linking may be facilitated in situ. Furthermore, we showed that gal-1 binding to the glycan Davanat attenuates inter-glycan interactions, a finding that may have biological consequences and deserves further investigation. Overall, these studies expand our view of how galectins in general may interact with more complex glycans on the extracellular matrix or cell surface.

## Material and methods

### *Galectin-1 preparation*

Uniformly $^{15}$N-labeled human galectin-1 was expressed in BL21(DE3) competent cells (Novagen), grown in minimal media, purified over a B lactose affinity column, and further fractionated on a gel filtration column, as described previously by Nesmelova, Pang, et al. (2008). Typically, 44 mg of purified protein were obtained from 1 L of cell culture. The purity of the final sample was quantified by using the Biorad protein assay and was checked for purity by using SDS–PAGE. Functional activity of the purified protein was assessed by using a T-cell death assay.

### *Glycan preparation*

The size reduction, isolation, and purification procedures for Davanat from commercially available *Cyamopsis tetragonoloba* guar gum flour were performed essentially as previously reported (Platt et al. 2006). Briefly, the procedure has five principal steps: (1) aqueous extraction of galactomannans, (2) controlled partial depolymerization, (3) recovery as an insoluble copper complex, (4) recovery from the copper complex, and (5) repeated ethanol precipitations. The final yield of Davanat was typically 50% by weight of guar gum flour. The purification procedure results in a pure Davanat as a white powder with a solubility in water of more than 60 mg/mL and a mannose:galactose ratio of 1.7. $^{1}$H-NMR and $^{13}$C-NMR spectra of Davanat are described in Platt et al. (2006).

Lactose and mannan (weight-averaged molecular weight of 50 kDa, derived from *Saccharomyces cerevisiae*) were purchased from Sigma Chemical and were used without further purification.

### *Heteronuclear NMR spectroscopy*

Uniformly $^{15}$N-labeled galectin-1 was dissolved at a concentration of 2 mg/mL in 50 mM sodium phosphate buffer at pH 7.0, made up using a 95% $H_2O$/5% $D_2O$ mixture. Using uniformly $^{15}$N-enriched gal-1, we performed HSQC NMR experiments to investigate binding of gal-1 to Davanat. $^{1}$H and $^{15}$N resonance assignments for recombinant human galectin-1 were already reported (Nesmelova, Pang, et al. 2008).

All NMR experiments were carried out at 30°C on a Varian Unity Inova 600 MHz spectrometer equipped with an H/C/N triple-resonance probe and *x*/*y*/*z* triple-axis PFG unit. A gradient sensitivity-enhanced version of two-dimensional $^{1}$H-$^{15}$N HSQC was applied with 256 ($t1$) × 2048 ($t2$) complex data points in nitrogen and proton dimensions, respectively. Raw data were converted and processed by using NMRPipe (Delaglio et al. 1995) and were analyzed by using NMRview (Johnson and Blevins 1994).

### *Pulsed field gradient NMR self-diffusion measurements*

For NMR diffusion measurements, Davanat was dissolved in 0.6 mL of potassium phosphate buffered $D_2O$, and the pH was adjusted by adding microliter quantities of NaOD or DCl. PFG NMR self-diffusion measurements were made on a Varian INOVA-600 using a GRASP gradient unit, as previously described (Mayo et al. 1996). NMR spectra for measurement of diffusion coefficients, $D$, were acquired using a 5 mm triple-resonance probe equipped with an actively shielded z-gradient coil. The maximum magnitude of the gradient was calibrated using the manufacturer's standard procedure based on the frequency spread of the applied gradient and was found to be 100 G/cm. This was consistent with the value of 98 G/cm obtained from analysis of PFG data on water using its known diffusion constant (Mills 1973). The linearity of the gradient was checked by performing diffusion measurements on water over different ranges of the gradient. The PFG longitudinal eddy-current delay pulse-sequence (Mayo et al. 1996) was used

for self-diffusion measurements which were performed in $D_2O$ at a temperature range 30°C.

For unrestricted diffusion of a molecule in an isotropic liquid, the PFG NMR signal amplitude, $A$, normalized to the signal obtained in the absence of gradient pulses, is related to $D$ by

$$A = \exp[-\gamma^2 g^2 \Delta^2 D(\Delta - \delta/3)] \quad (1)$$

where $\gamma$ is the gyromagnetic ratio of the observed nucleus; $g$ and $\delta$ are the magnitude and duration of the magnetic field gradient pulses, respectively, and $\Delta$ is the time between the gradient pulses (Mills 1973). For these experiments, $\delta = 4$ ms, $g = 1$ – 75 G/cm, $\Delta = 34.2$ ms, and the longitudinal eddy-current delay $T_e = 100$ ms. Each diffusion constant, $D$, was determined from a series of 12 one-dimensional PFG spectra acquired using different $g$-values. Diffusion coefficient measurements were calibrated by performing the PFG NMR self-diffusion measurements on dextran standards and standard proteins (Ilyina et al. 1997; Miller, Klyosov, et al. 2009).

## Funding

The National Cancer Institute (NIH R01 CA096090 to K.H.M.); support from the National Institutes of Health Cancer Biology Training Grant (NIH T32 CA009138) to M.C.M.; the National Science Foundation (BIR-961477); the University of Minnesota Medical School; the Minnesota Medical Foundation.

## Acknowledgements

We are most grateful and indebted to Professor Linda Baum and Mabel Pang of the Department of Pathology and Laboratory Medicine, UCLA for providing us with isotopically enriched recombinant human gal-1, as well as for reading the manuscript and for many help comments and suggestions.

## Conflict of interest statement

Dr. Klyosov has a significant financial interest in Pro-Pharmaceuticals, Inc., which owns the rights to Davanat.

## Abbreviations

CRD, carbohydrate recognition domain; Davanat, preparation of a Guar gum-derived galactomannan trademarked as DAVANAT®; gal-1, galectin-1; HSQC, heteronuclear single quantum coherence; NMR, nuclear magnetic resonance; PFG, pulse field gradient.

## References

Appukuttan PS. 2002. Terminal α-linked galactose rather than *N*-acetyl lactosamine is ligand for bovine heart galectin-1 in *N*-linked oligosaccharides of glycoproteins. *J Mol Recogn.* 15:180–187.

Appukuttan PS, Geetha M, Annamma KI. 1995. Anomer specificity of the 14 kDa galactose binding lectin, a reappraisal. *J Biosci.* 20:377–384.

Balcan E, Tuglu I, Sahin M, Toparlak P. 2008. Cell surface glycosylation diversity of embryonic thymic tissues. *Acta Histochem.* 100:14–25.

Barondes SH, Castronovo V, Cooper DN, Cummings RD, Drickamer K, Feizi T, Gitt MA, Hirabayashi J, Hughes C, Kasai K, et al. 1994. Galectins: A family of animal β-galactoside-binding lectins. *Cell.* 76:597–598.

Bourne Y, Bolgiano B, Liao DI, Strecker G, Cantau P, Herzberg O, Feizi T, Cambillau C. 1994. Crosslinking of mammalian lectin (galectin-1) by complex biantennary saccharides. *Nat Struct Biol.* 1:863–870.

Brewer CF, Miceli MC, Baum LG. 2002. Clusters, bundles, arrays, and lattices: Novel mechanisms for lectin-saccharide-mediated cellular interactions. *Curr Opin Struct Biol.* 12:616–623.

Cantor CR, Schimmel PR. 1980. The behavior of biological macromolecules. In: *Biophysical Chemistry, Part III*. New York: W. H. Freeman. p. 979–1039.

Daas PJH, Schols HA, de Jongh HHJ. 2000. On the galactosyl distribution of commercial galactomannans. *Carbohyd Res.* 329:609–619.

Daniels MA, Hogquist KA, Jameson SC. 2002. Sweet "n" sour: The impact of differential glycosylation on T cell responses. *Nat Immunol.* 3:903–910.

Delaglio F, Grzesiek S, Vuister GW, Zhu G, Pfeifer J, Bax A. 1995. NMRPipe: a multidimensional spectral processing system based on UNIX pipes. *J Biomol NMR.* 6:277–293.

Fischer C, Sanchez-Ruderisch H, Welzel M. 2005. Galectin-1 interacts with the α5β1 fibronectin receptor to restrict carcinoma cell growth via induction of p21 and p27. *J Biol Chem.* 280:37266–37277.

Fradin C, Poulain D, Jouault T. 2000. β-1,2-Linked oligomannosides from *Candida albicans* bind to a 32-kilodalton macrophage membrane protein homologous to the mammalian lectin galectin-3. *Infect Immun.* 68:4391–4398.

Fukuda M. 1996. Possible roles of tumor-associated carbohydrate antigens. *Cancer Res.* 56:2237–2244.

Gupta RK, Pande AH, Gulla KC, Gabius H-J, Hajela K. 2006. Carbohydrate-induced modulation of cell membrane: VIII. Agglutination with mammalian lectin galectin-1 increases osmofragility and membrane fluidity of trypsinized erythrocytes. *FEBS Lett.* 580:1691–1695.

Ikuta K, Shibata N, Blake JS, Dahl MV, Nelson RD, Hisamichi K, Kobayashi H, Suzuki S, Ohawa Y. 1997. NMR study of the galactomannans of *Trichophyton mentagrophytes* and *Trichophyton rubrum*. *Biochem J.* 323:297–305.

Ilyina E, Roongta V, Pan H, Woodward C, Mayo KH. 1997. A pulsed field gradient NMR study of bovine pancreatic trypsin inhibitor self-association. *Biochemistry.* 36:3383–3388.

Ishrud O, Zahid M, Zhou H, Pan Y. 2001. A water-soluble galactomannan from the seeds of *Phoenix dactylifera* L. *Carbohyd Res.* 335:297–301.

Johnson BA, Blevins RA. 1994. NMRview: A computer program for the visualization and analysis of NMR data. *J Biomol NMR* 4:603–614.

Kannagi R, Izawa M, Koike T, Miyazaki K, Kimura N. 2004. Carbohydrate-mediated cell adhesion in cancer metastasis and angiogenesis. *Cancer Sci.* 95:377–384.

Keeler J. 2005. *Understanding NMR Spectroscopy*. New York: Wiley.

Kohatsu L, Hsu DK, Jegalian AG, Liu FT, Baum LG. 2006. Galectin-3 induces death of *Candida* species expressing specific β-1,2-linked mannans. *J Immunol.* 177:4718–4726.

Laughlin ST, Baskin JM, Amacher SL, Bertozzi CR. 2008. In vivo imaging of membrane-associated glycans in developing Zebrafish. *Science.* 320:664–667.

Liu FT, Rabinovich GA. 2005. Galectins as modulators of tumour progression. *Nat Rev Cancer.* 5:29–41.

Lopez-Lucendo MF, Solıs D, Andre S, Hirabayashi J, Kasai K, Kaltner H, Gabius H-J, Romero A. 2004. Growth-regulatory human galectin-1: Crystallographic characterisation of the structural changes induced by single-site mutations and their impact on the thermodynamics of ligand binding. *J Mol Biol.* 343:957–970.

Mayo KH, Ilyina E, Park H. 1996. A recipe for designing water soluble β-sheet-forming peptides. *Protein Sci.* 5:1301–1315.

Mikhailov D, Young HC, Linhardt RJ, Mayo KH. 1999. Heparin dodecasaccharide binding to platelet factor-4 and growth-related protein-alpha. Induction of a partially folded state and implications for heparin-induced thrombocytopenia. *J Biol Chem.* 274:25317–25329.

Miller M, Klyosov A, Platt D, Mayo KH. 2009. Using pulse field gradient NMR diffusion measurements to define molecular weight distributions in glycan preparations. *Carbohyd Res.* 344:1205–1212.

Miller MC, Nesmelova IV, Platt D, Klyosov A, Mayo KH. 2009. Carbohydrate binding domain on galectin-1 is more extensive for a complex glycan than for simple saccharides: Implications for galectin–glycan interactions at the cell surface. *Biochem J.* 421:211–221.

Mills R. 1973. Molecular diffusion. *J Phys Chem*. 77:685–688.

Nagae M, Nishi N, Murata T, Usui T, Nakamura T, Wakatsuki S, Kato R. 2006. Crystal structure of the galectin-9 N-terminal carbohydrate recognition domain from Mus musculus reveals the basic mechanism of carbohydrate recognition. *J Biol Chem.* 281:35884–35893.

Neri D, Bicknell R. 2005. Tumour vascular targeting. *Nat Rev Cancer.* 5:436–446.

Nesmelova IV, Dings RPM, Mayo KH. 2008. Understanding galectin structure–function relationship to design effective antagonists. In: Klyosov AA, Witczak ZJ, Platt D, editors. *Galectins*. John Wiley & Sons, Hoboken, New Jersey. p. 33–69.

Nesmelova IV, Pang M, Baum LG, Mayo KH. 2008. $^{1}$H, $^{13}$C, and $^{15}$N backbone and side-chain chemical shift assignments for the 29 kDa human galectin-1 protein dimer. *J NMR Assign.* 2:203–205.

Nieminen J, Kuno A, Hirabayashi J, Sato S. 2007. Visualization of galectin-3 oligomerization on the surface of neutrophils and endothelial cells using fluorescence resonance energy transfer. *J Biol Chem.* 282:1374–1383.

Pace KE, Lee C, Stewart LG, Baum LG. 1999. Restricted receptor segregation into membrane microdomains occurs on human T cells during apoptosis induced by galectin-1. *J Immunol.* 163:3801–3811.

Perillo NL, Pace KE, Seilhamer JJ, Baum LG. 1995. Apoptosis of T cells mediated by galectin-1. *Nature.* 378:736–739.

Perillo NL, Uittenbogaart CH, Nguyen JT, Baum LG. 1997. Galectin-1, an endogenous lectin produced by thymic epithelial cells, induces apoptosis of human thymocytes. *J Exp Med.* 185:1851–1858.

Platt D, Klyosov AA, Zomer E. 2006. In: Klyosov AA, Witczak ZJ, Platt D, editors. *Carbohydrate Drug Design*. ACS Symposium Series 932. American Chemical Society, Washington, DC. p. 49–66.

Rabinovich GA, Toscano MA, Jackson SS, Vasta GR. 2007. Functions of cell surface galectin–glycoprotein lattices. *Curr Opin Struct Biol.* 17:513–520.

Rabuka D, Forstner MB, Groves JT, Bertozzi CR. 2008. Noncovalent cell surface engineering: Incorporation of bioactive synthetic glycopolymers into cellular membranes. *J Am Chem Soc.* 130:5947–5953.

Rabuka D, Parthasarathy R, Lee GS, Chen X, Groves JT, Bertozzi CR. 2007. Hierarchical assembly of model cell surfaces: Synthesis of mucin mimetic polymers and their display on supported bilayers. *J Am Chem Soc.* 129:5462–5471.

Rajagopal P, Waygood EB, Reizer J, Saier MH, Klevit RE. 1997. Demonstration of protein–protein interaction specificity by NMR chemical shift mapping. *Protein Sci.* 6:2624–2627.

Rakhmanberdyeva RK, Shashkov AS. 2005. Structure of galactomannans from *Gleditsia delavayi* and *Gleditsia aquatica* by $^{1}$H and $^{13}$C NMR spectroscopy. *Chem Nat Compd.* 41:14–22.

Rodgers KD, San Antonio JD, Jacenko O. 2008. Heparan sulfate proteoglycans: A GAGgle of skeletal-hematopoietic regulators. *Dev Dyn.* 237:2622–2642.

Swaminathan GJ, Leonidas DD, Savage MP, Ackerman SJ, Acharya KR. 1999. Selective recognition of mannose by the human eosinophil Charcot-Leyden crystal protein (galectin-10): A crystallographic study at 1.8 A resolution. *Biochemistry.* 38:13837–13843.

Taguchi T, Muto Y, Kitajima K, Yokoyama S, Inoue S, Inoue Y. 1997. Proton NMR study of triantennary type *N*-linked glycan chains: Assignment of proteonchemical shifts of the β-Man residue in a basic unit of the triantennary glycan chain. *Glycobiology.* 7:31–36.

Takita J, Katohda S, Sugiyama H. 2001. Structural determination of an exocellular mannan from *Rhodotorula mucilaginosa* YR-2 using ab initio assignment of proton and carbon NMR spectra. *Carbohyd Res.* 335:133–139.

Taylor ME, Drickamer K. 2007. Paradigms for glycan-binding receptors in cell adhesion. *Curr Opin Cell Biol.* 19:572–577.

Thijssen VL, Postel R, Brandwijk RJ, Dings RP, Nesmelova I, Satijn S, Verhofstad N, Nakabeppu Y, Baum LG, Bakkers J, et al. 2006. Galectin-1 is essential in tumor angiogenesis and is a target for antiangiogenesis therapy. *Proc Natl Acad Sci USA.* 103:15975–15980.

Walser PJ, Haebel PW, Kunzler M, Sargent D, Kues U, Aebi M, Ban N. 2004. Structure and functional analysis of the fungal galectin CGL2. *Structure.* 12:689–702.

Werz DB, Ranzinger R, Herget S, Adibekian A, von der Lieth C-W, Seeberger PH. 2007. Exploring the structural diversity of mammalian carbohydrates ("glycospace") by statistical databank analysis. *Chem Biol.* 2:685–691.

Wu AM, Singh T, Wu JH, Lensch M, Andre S, Gabius H-J. 2006. Interaction profile of galectin-5 with free saccharides and mammalian glycoproteins: Probing its fine specificity and the effect of naturally clustered ligand presentation. *Glycobiology.* 16:524–537.